

Experimental Investigation of Depth Cues for Small-Field Light Sources in Darkness

Yuko Harada¹, Midori Tanaka², Takahiko Horiuchi²

¹Graduate School of Science and Engineering, Chiba University, Chiba, Japan; ²Graduate School of Informatics, Chiba University, Chiba, Japan

E-mail: 24wm3211@student.gs.chiba-u.jp

Abstract. In recent years, the effects of light pollution have become significant, and the need for image reproduction of a faithful and preferred starry sky has increased. Previous studies have analyzed the relationships between the luminance, size, and color temperature of stars and the fidelity and nature of their appearance, as well as color perception. This study examines the depth perception of stars. We consider starry sky images as a set of “small-field light sources” that can be viewed as point light sources with minimal viewing angles. Our goal was to experimentally elucidate the cues for depth perception. In our experiments, observers viewed two points of different sizes, luminances, and color temperatures and selected the one perceived to be in front to confirm the relationship between the three depth cues of retinal image; size, light attenuation, and color, and their association with depth perception. Results confirmed that retinal image size and light attenuation were relevant for a small-field light source. Results also suggest that the interaction between retinal image size and light attenuation may be explained by retinal illuminance. However, the effect of color was small, and the point with higher saturation was more likely to be perceived in front, when the hue was close to that of the point.

Keywords: point light source, depth perception, image reproduction, star, retinal illuminance, color temperature

© 2024 Society for Imaging Science and Technology.

[DOI: 10.2352/J.Percept.Imaging.2024.7.000405]

1. INTRODUCTION

The advancement of civilization has brought about the problem of light pollution, which is caused by light emitted from lighting fixtures leaking in unintended directions and is characterized as being of inappropriate luminance or color for the surrounding environment, or present even when it is not needed. Light pollution occurs all over the world. A light pollution map [19], which shows the severity of light pollution by color, indicates that the effects are spread throughout the world, centering on major cities, such as London, New York, and Shanghai. An unintended consequence of the effects of lighting is the difficulty in observing stars. As a result, the demand for planetariums that artificially reproduce the images and motion of stars in a dome is increasing [5, 16]. Planetariums not only play an educational role in geology and astronomy by making them

more accessible, but also a historical role in documenting the night sky of each era with a higher degree of reproducibility than that of photographs or videos [4], and a recreational role in making the starry sky viewable even in urban areas where light pollution is substantial. The increasing demand for planetariums requires the projection of highly accurate star images to the dome.

Starry sky image reproduction methods are classified into two types: faithful starry sky reproduction, which aims to achieve a representation equivalent to the actual space; and preferred starry sky reproduction, which allows a variation from the actual space for a more human-preferred reproduction. Using a digital planetarium, Sawada et al. projected the night sky at different naked-eye-limiting magnitudes and concluded that observers living in areas susceptible to light pollution tended to rate the fidelity of the starry sky as high, even when the naked-eye-limiting magnitude was low [16]. Tanaka et al. experimented with an optical planetarium to reproduce a starry sky using an evaluation formula of the observer and determined that changes in luminance affected fidelity more strongly than changes in size or color temperature [20]. They also examined the relationship between fidelity and preference for star fields in planetariums through psychometric experiments and determined that male observers sought faithful star reproductions as their preferred reproductions. Female observers, on the other hand, did not find faithful star reproductions desirable and rated more brilliant star reproductions as desirable. These results were not influenced by their experience with astronomical observations [21]. Additionally, studies on the visual fidelity of Milky Way have shown that star density is also an important factor [22]. However, despite the significant difference between the reproduction of the night sky within a dome and the actual night sky in terms of the sense of distance and depth between stars, the relationship between depth perception and reproduction of the night sky has not been sufficiently elucidated.

Starry sky images can be viewed as point-light sources because of their minimal viewing angle; however, unlike ideal point-light sources, they are of a specific size. For simplicity, this study refers to such a light source a “small-field light source.” When a small-field light source is observed, light stimuli are perceived in the central pit, which is located

Received July 23, 2024; accepted for publication Nov. 16, 2024; published online Dec. 13, 2024. Associate Editor: Damon Chandler.

2575-8144/2024/7/000405/11/\$00.00

further inward than fovea centralis, and since there are no S-cones in the central pit, color perception traits such as tritanopia, a type of color blindness, can occur. This phenomenon is referred to as small-field tritanopia [13]. In an experiment by Ogawa et al., color temperatures of 5400 K and 11600 K were perceived as similar to tritanopia, while the color temperature of 3500 K was perceived as similar to protanopia, i.e., the absence of L-cones, indicating that the perception of small-field light sources remains unclear [14]. Robert et al. proposed that light scattering in the eye interacts multiplicatively with cone-induced attenuation of color perception based on empirical experiments in the range of $1/8^\circ$ to 2° of visual field angles [3]. Furthermore, small-field light sources are difficult to be perceived accurately, and their size and brightness are perceived by point spread function (PSF) [24]. Since small-field light sources have different characteristics than ordinary light sources, it is necessary to consider the possibility that they also have more depth characteristics than the depth perception of illuminated objects or the entire visual field.

Various models for estimating depth have been considered in depth perception research, among which the weighted linear combination model elucidates several phenomena [11]. This model posits that brain perceives depth through a weighted averaging process of information which results from the integration of outputs from various processing systems corresponding to different depth cues. However, the specific integration methods and interrelationships among these cues remain unclear, thus prompting ongoing research on the perceptions that arise when multiple depth cues are integrated. Ichikawa et al. investigated the depth perception of different cues such as motion parallax, binocular parallax, and shape and determined that the brain perceives depth from different cues at different stages of visual processing [8]. Johnston et al. investigated the interaction between stereopsis and shape perception based on texture and concluded that these cues do not act independently [10]. However, most of these studies were conducted on the visibility of images, such as shapes and volumes, and there have been no experiments on the depth perception of light sources, especially small-field light sources.

Our study focused on retinal image size and light attenuation for achromatic small-field light sources and confirmed their effects and interrelationships. We introduced color as a depth cue and analyzed its effects, the interrelationship between color and retinal image size, and the interrelationship between color and light attenuation. Specifically, we examined the cues that affect depth perception between small-field light sources through experiments using two-alternative forced choice (2AFC) between two small-field light sources with multiple cues. The experiment was conducted with one eye, as binocular depth cues are negligible in distant observation conditions typical of stars or planetariums.

2. DEPTH PERCEPTION CUES

Human depth perception relies on various cues which can be classified according to several criteria. We use the classification method posited by Fatima et al. [9], which includes proprioceptive, monocular, binocular, and dynamic cues. Proprioceptive cues are based on the physiological responses of eye receptors. Examples include accommodation, which is a function of lens thickness adjustment and convergence angle. Monocular cues enable a single eye to perceive depth. Examples include occlusion, size of retinal images, aerial perspective, shading, light attenuation, and linear perspective. Binocular cues, also called stereopsis, are derived from the difference in projected position on retina due to the difference in the position of left and right eyes. Dynamic cues are derived from information that changes as an observer moves or rotates and are called motion parallax.

Depth cues that contribute to starry sky observation are limited to a subset of these cues. Proprioceptive cues only function for short or intermediate distances. At long distances, the retinal images projected to left and right eyes can be considered as identical; therefore, binocular cues do not function. While dynamic cues can be used as an index for depth comparison with the foreground, they do not provide a sense of depth between star images. Therefore, it is necessary to focus solely on monocular cues. Palmisano et al. determined that size is an important factor for obtaining a sense of distance when an object is far away [15]. Light attenuation is also an important cue because illuminance decreases in proportion to the square of the distance. Color is also an indicator of small-field light sources with low information content. Regarding depth perception and color, red is perceived as being closest in distance and blue as the farthest, a phenomenon known as retreating and advancing color [12].

Based on literature evidence, this study addresses three depth cues: retinal image size, light attenuation, and color, which are referred to as size, luminance, and color temperature, respectively.

3. EXPERIMENTS

3.1 Environment

Figure 1 depicts the experimental room environment. Fig. 1(a) displays a photograph and Fig. 1(b) illustrates a schematic of the display. Observers were seated at 2.5 m from the display and rested their heads on a chinrest. The distance of 2.5 m was chosen because accommodation, one of the depth cues, only functions effectively at extremely short distances (less than 2 m). A cloth was used to cover the chinrest to conceal one eye and the observer watched the small-field light source using only the eye with best visual acuity. Use of single eye eliminated the influence of depth cues such as convergence and stereopsis. The distance between the points was 4° in angle of view and 18.8 cm in length. All experiments were conducted in a dark room. The entire display was covered with a blackout curtain to prevent the observer from being influenced by other light sources. A

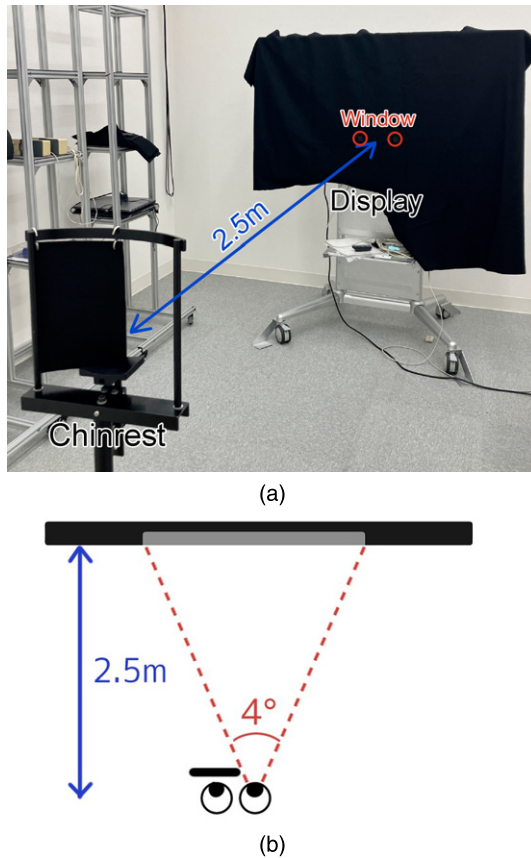


Figure 1. Experimental environments. (a) Photograph. (b) Schematic diagram.

hole with a radius of 2 cm was created to expose only the light source.

3.2 Procedure

3.2.1 Experiment 1: Size and Luminance

In Experiment 1, the effects and interrelationships of the size and luminance of achromatic small-field light sources on depth perception were investigated using 2AFC. Nine male and female observers in their 20 s with normal color vision participated in this experiment. The observers' visual acuity ranged from a minimum of 0.3 to a maximum of 1.5, with an average of 1.1. Even at minimum acuity, they resolved the smallest points among the experimental stimuli. Figure 2 illustrates the experimental procedure. The experiment was conducted in a dark room to simulate the conditions for observing star images. Since the stimulus with the lowest luminance is approximately 0.6 cd/m^2 , at which point rod adaptation is not required, the dark-adaptation period was approximately 10 min. The observer viewed two achromatic dots of different luminances and sizes on a 133 cm (W) \times 75 cm (H) display (Sharp PN-A601) with a 60 V wide TFT LCD. Figure 3 depicts a small-field light-source stimulus input on the display, from which the observer must select the stimulus perceived to be in the foreground. Even if the depths of the left and right points were perceived to be equal, the observer was asked to select one of them. Once a stimulus was selected, the observer was shown the next stimulus on

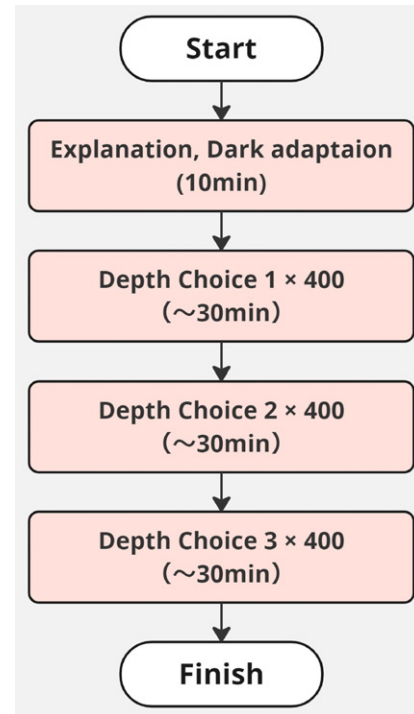


Figure 2. Flowchart of Experiment 1.

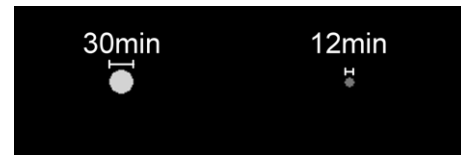


Figure 3. An example of a pair of stimuli with different size and luminance.

the display, and the experiment was repeated several times. Three sets of 400 stimulus pairs were used in this experiment, totaling 1200 pairs. Each observer took one to three seconds per selection.

Two small-field light sources were shown to the observers, one of which was a reference point with fixed size and luminance, and the other was a randomly determined comparison point. These points were used to determine the thresholds for points perceived to be either in front or behind relative to a reference point. The experiments were conducted using three reference points.

Figure 4 shows a scatterplot of luminance (L^*) and diameter (viewing angle) of the reference and comparison points. L^* was calculated using a white point with a luminance of 100 cd/m^2 on the display, with $L^* = 100$ set as the white reference. The visual angle varied from 3 arcminutes, which is the display limit, to 30 arcminutes, corresponding to the size of the moon. The three black triangles in Fig. 4 indicate the reference points and their respective values are listed in Table I. For simplicity, these points are labeled as 1, 2, and 3. The comparison points were the same, regardless of the reference point values, and the observers were asked to choose the point which appeared

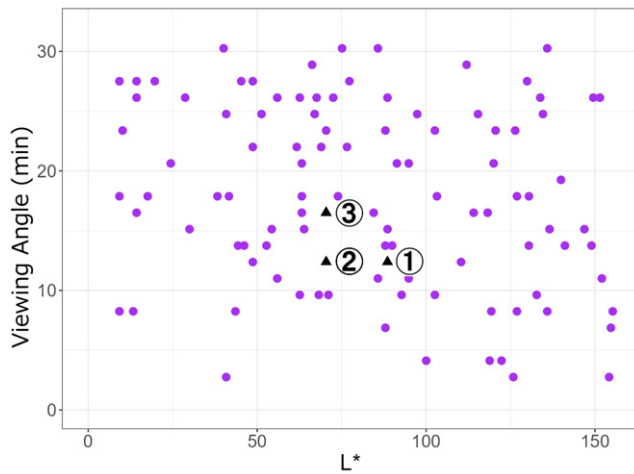


Figure 4. Stimuli of Experiment 1.

Table 1. Luminance and size of reference points.

Reference point	Luminance L^*	Viewing angle (min)
1	88.58	12.4
2	70.42	12.4
3	70.42	16.5

closer for a total of 300 pairs of stimuli images (3 reference points \times 100 comparison points). For each combination, observers made four selections: twice when the reference point was on the left and twice when the reference point was on the right; the number of times when the observer selected the comparison point as the closer one was recorded. The depth choices of 1, 2, and 3 shown in the flowchart (Fig. 2) indicate that the experiment was conducted using a separate set of images for each reference point.

3.2.2 Experiment 2: Color

In Experiment 2, the effects of color temperature on depth perception of small-field light sources and their interrelationships with size and brightness were investigated using 2AFC. Ten male and female observers in their 20 s with normal color vision participated in this experiment, including nine of those who participated in Experiment 1. Figure 5 depicts the experimental procedure. Similar to Experiment 1, Experiment 2 was also conducted in a dark room to simulate the conditions for observing star images; as the stimulus with the lowest luminance is approximately 5 cd/m^2 , at which point rod adaptation is not required, the dark adaptation period was approximately 10 min. The observers participated in luminance and color temperature experiment, followed by size and color temperature experiment. The observers viewed two points of different sizes and color temperatures, or luminances and color temperatures, on the same display which was

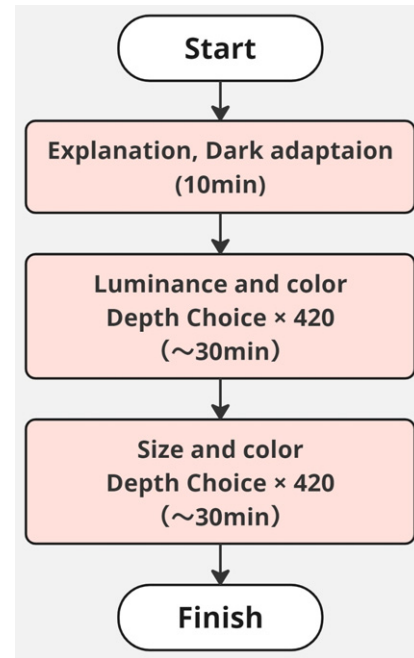


Figure 5. Flowchart of Experiment 2.

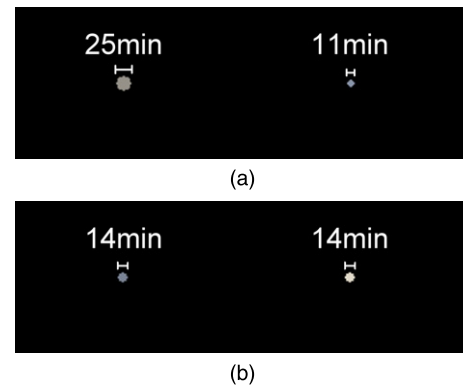
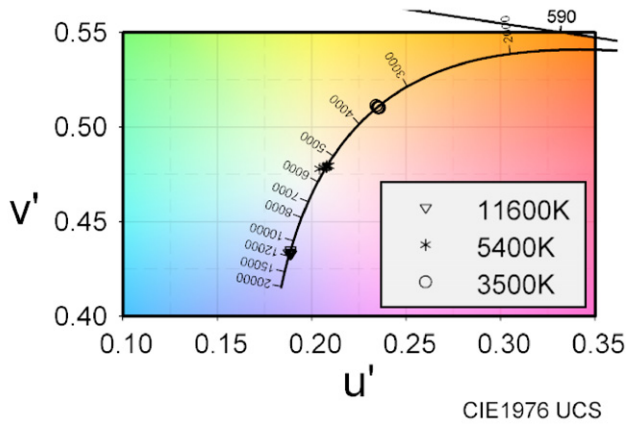


Figure 6. Examples of a pair of stimuli with different color temperatures. (a) Two points of different sizes and color temperatures. (b) Two points of different luminance and color temperatures.

used in Experiment 1. Figure 6 shows the small-field light source stimulus input on the display. Fig. 6(a) shows the differences in size and color temperature, and Fig. 6(b) shows the differences in luminance and color temperature. 420 stimulus pairs were used for luminance and color temperature experiment as well as for size and color temperature experiment, totaling 840 pairs. Each observer took one to three seconds per selection.

The color temperatures of the stimuli were 3500 K (color temperature of Betelgeuse), 5400 K (color temperature of Capella), and 11600 K (color temperature of Rigel). These color temperatures were selected from the blackbody radiation locus as stars whose temperatures (low, medium, high) are approximately equidistant on the CIE 1976 $u'v'$ uniform chromaticity diagram. Each color temperature was adjusted using a spectroradiometer (Konica Minolta CS-2000) to target the following values: 3500 K $(x, y) =$

Figure 7. $u'v'$ color map for Experiment 2.

(0.404, 0.390), 5400 K (x, y) = (0.334, 0.343), and 11600 K (x, y) = (0.273, 0.280). Figure 7 shows the experimental stimuli plotted on a $u'v'$ chromaticity diagram. Since the input RGB values could only be controlled from 0 to 255 and had to approach the desired chromaticity while adjusting the luminance, slight errors were observed, particularly at lower brightness levels. However, these values were within the acceptable range for the experiment.

Table II shows specifications of Experiment 1 which examined the relationship between size and color temperature; each color temperature had a luminance of $L^* = 89.8$ and five different sizes, as shown in Table II(a). These small-field light sources are labeled as Stimulus 1 for simplicity. In the experiment examining the relationship between luminance and color temperature, each color temperature had a viewing angle of 12.4 min and five different luminance values, as listed in Table II(b). These small-field light sources are labeled Stimulus 2 for simplicity.

In both Stimulus 1 and 2, all possible combinations of two points from 15 small-field light sources were used for 2AFC. The observers were asked to choose the image that appeared closer for a total of ${}_{15}C_2 = 210$ pairs of stimuli images. For each combination, observers made four selections, switching left and right, and the number of times the observers selected a comparison point as the closer one was recorded.

4. RESULTS AND CONSIDERATIONS

4.1 Experiment 1: Size and Luminance

4.1.1 Results

Figure 8 summarizes the results of all nine observers for each reference point; for all depth selections, the minimum time for one set was 10 min, the maximum was 30 min, and the average was 15 min. Fig. 8(a), Fig. 8(b) and Fig. 8(c) show the results of the experiment with reference points 1, 2 and 3, respectively, where the number of selections ranged from 0 to 36. The points plotted with black triangles indicate the reference points and those plotted with circles are the comparison points. The color of the comparison points is differentiated based on the number of times they

Table II. Specifications of Experiment 1. (a) Stimulus 1 parameters. (b) Stimulus 2 parameters.

(a)					
L^*	89.8				
Viewing Angle (min)	6.9	9.6	12.4	15.1	17.9
(b)					
L^*	28.8	48.9	79.8	108	136
Viewing Angle (min)	12.4				

were selected as 'perceived in front than the reference point,' with more frequent selections denoted in red and less frequent selections in blue. Gray, an intermediate color, can be perceived in either direction or as the scenario in which the depth of the image equals that of the reference point.

The green line indicates the threshold for points perceived as being in front of or behind the reference point, determined with a support vector machine (SVM). The results were binarized by defining points which were selected as being in the foreground more than 50% of the time as 1 and those selected less than 50% of the time as 0. This classification was performed with a polynomial kernel. The slope of the line decreased with increasing L^* and changed when $L^* = 50$ at reference points 1 and 3 because there was no comparison point near (L^* , viewing angle (min)) = (40, 30); when assuming that there is a point where the selection ratio is less than 50%, the classification line would be close to reference point 2. There was no correlation between visual acuity and the results for either stimulus.

4.1.2 Considerations

The neighboring points of a line parallel to the viewing-point axis passing through the reference point represent points of equal size but of different luminances. Focusing on these points from the perspective of the effect of size on the depth perception of a small-field light source, a larger light source is perceived as being in front, conversely, a smaller light source is perceived as being behind. This result is consistent with the feature of retinal image size, the larger the image on the retina, the more it is perceived to be in the foreground. The neighboring points of a line parallel to L^* axis passing through the reference point represent points of equal size but of different luminances. Analyzing these points to examine the effect of brightness on depth perception of small-field light sources, it can be inferred that points with brighter light are perceived as being in front, whereas darker ones are perceived as being behind. This result is consistent with the feature of light attenuation, when light at a greater distance appears darker.

Next, we consider the relationship between the size and luminance in the depth perception of small-field light sources.

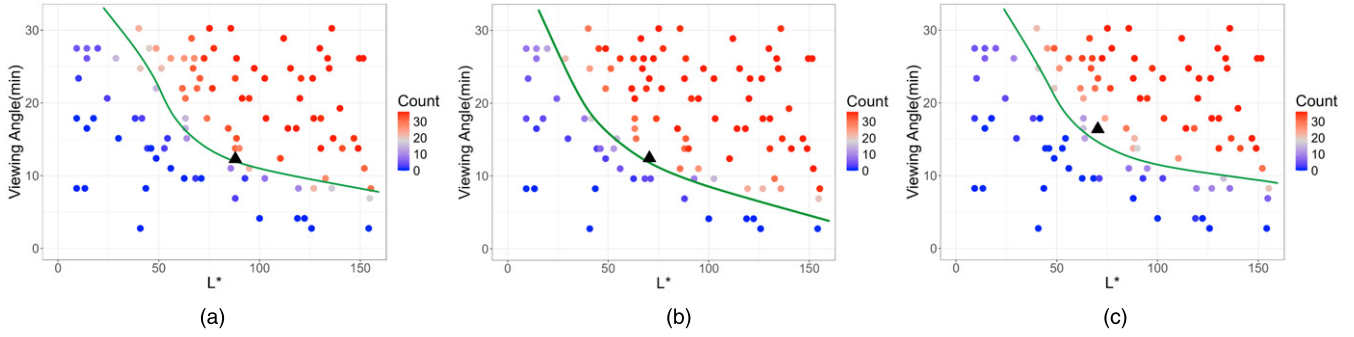


Figure 8. Results of Experiment 1. (a) Observations pertaining to reference point 1. (b) Observations pertaining to reference point 2. (c) Observations pertaining to reference point 3.

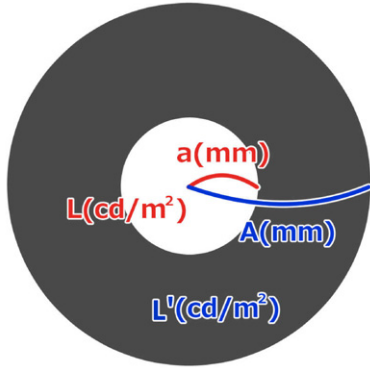


Figure 9. Average luminance.

As the binary classification line is curved, the predominance of retinal image size or light attenuation could not be ascertained. However, several studies report that the total amount of light reflected from the eye influenced the selection.

We analyzed the relationship between retinal illuminance, a photometric quantity representing illuminance on the retinal surface, and the experimental results. The magnitude of retinal illuminance determined depth perception. When viewing a surface with luminance L (cd/m^2) through a pupil of radius r (mm), the retinal illuminance $E_r(td)$ can be expressed as:

$$E_r = \pi \cdot r^2 \cdot L. \quad (1)$$

We determined the retinal illuminance of a small-field light source with luminance L (cd/m^2) and radius a (mm). Initially, as the luminance of a small-field light source differs from that of an extended source, L is not directly substituted into Eq. (1) and the average of the surrounding luminance L' is computed. The area of the extended source projected onto the retina was considered as a circle with radius A (mm). A schematic of this process is shown in Figure 9. Eq. (2) expresses the luminous intensity I within a circle:

$$I = \pi 10^{-6} [La^2 + \{L'(A^2 - a^2)\}]. \quad (2)$$

Thus, the average L_{ave} of the surrounding luminance of a small-field light source can be calculated as follows:

$$E_r = \pi r^2 \left\{ (L - L') \frac{a^2}{A^2} + L' \right\}. \quad (3)$$

We consider a reference point with luminance L_0 (cd/m^2) and radius a_0 (mm) observed through a pupil diameter r_0 (mm). Using Eq. (3), the luminance L and radius a of a small-field light source with a retinal illuminance equal to $E_{r0}(td)$ can be calculated.

$$\begin{aligned} \pi r^2 \left\{ (L - L') \frac{a^2}{A^2} + L' \right\} &= E_{r0} \\ \pi r^2 \left\{ (L - L') \frac{a^2}{A^2} + L' \right\} &= \pi r_0^2 \left\{ (L_0 - L') \frac{a_0^2}{A^2} + L' \right\} \\ a &= A \sqrt{\left(\frac{r_0}{r} \right)^2 \left\{ \frac{L_0 - L'}{L - L'} \left(\frac{a_0}{A} \right)^2 + \frac{L}{L - L'} \right\} - \frac{L'}{L - L'}}. \end{aligned} \quad (4)$$

Experimental results show that under $1lx$ illumination, the pupil diameter ranged between 4 mm and 9 mm [2], and under illumination of 0 (cd/m^2), it ranged between 4 mm and 6 mm [23]. As it is impossible to conduct the experiment and measure the pupil diameter simultaneously and since values vary significantly from person to person, this study assumes that the pupil diameter r varies with the luminous intensity of small-field light source. When the luminance and radius of the reference point are L_0 (cd/m^2) and a_0 (mm), respectively, the luminous intensity I_0 of the reference point is calculated as follows:

$$I_0 = L_0 \cdot \pi \left(10^{-3} a_0 \right)^2. \quad (5)$$

The function of radius a and luminance L of a point that has the same luminous intensity as this point is as follows:

$$a = \sqrt{\frac{L_0}{L}} a_0. \quad (6)$$

Figure 10 illustrates the function of L^* and the viewing angle for points with same luminous intensity as the reference

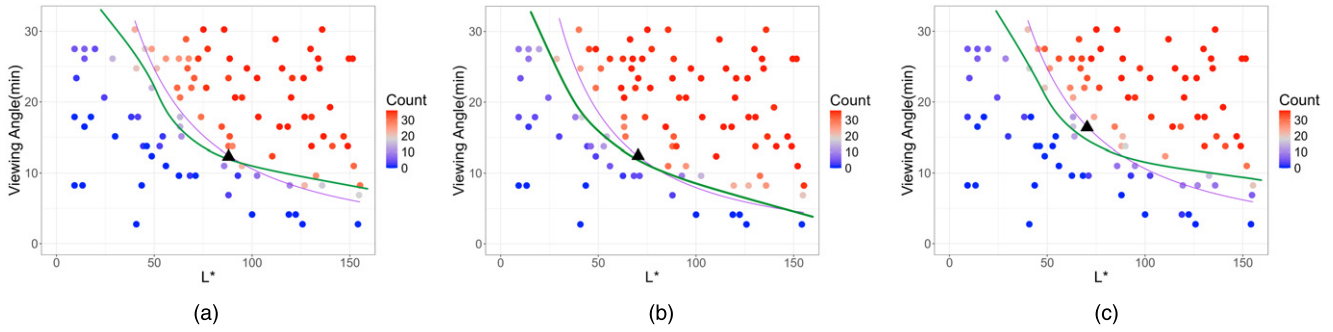


Figure 10. Identical luminous intensity function. (a) Observations pertaining to reference point 1. (b) Observations pertaining to reference point 2. (c) Observations pertaining to reference point 3.

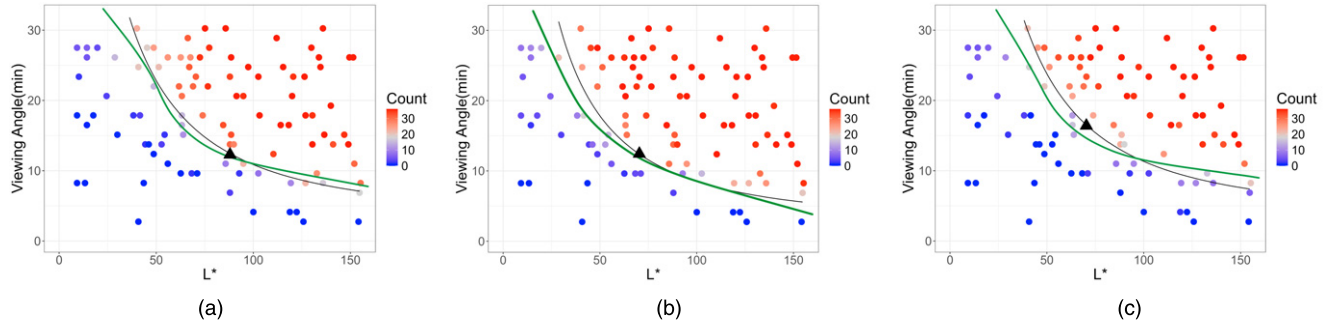


Figure 11. Identical retinal illuminance function. (a) Observations pertaining to reference point 1. (b) Observations pertaining to reference point 2. (c) Observations pertaining to reference point 3.

point determined using Eq. (6) (purple in Fig. 8). Fig. 10 indicates that the luminous intensity is greater than that of the reference point for a larger viewing angle, and smaller for a smaller viewing angle. Fig. 10(a) corresponds to reference point 1; Fig. 10(c) corresponds to point 3. The values along the binary classification line obtained using SVM show that the luminous intensity is lower than the reference point for lower L^* values and higher for higher L^* values. Fig. 10(b) corresponds to reference point 2, and the values along the binary classification line obtained using SVM similarly indicate that the luminous intensity decreases as L^* decreases. However, at higher L^* values, the luminous intensity is almost equal to that of the reference point.

It can be inferred from these results that L^* determines the difference in luminous intensity between the threshold and reference point. Moreover, assuming that the pupil diameter changes with the luminous intensity of small-field light sources, we can conclude that a lower L^* results in a larger pupil diameter, owing to lower luminous intensity, and a higher L^* results in a smaller pupil diameter, due to higher luminous intensity. Reiterating the inability to measure pupil diameter simultaneously with the experiment, this study assumed a linear change in pupil diameter between 6–8 mm within the $L^* \geq 25$ range for subsequent calculations. This range was chosen based on the experiment by Bradley et al. [2], which determined that the pupil diameter tends to decrease with age. The pupil diameter of observers in their 20s in this experiment ranged from 5.7 mm to 8.8 mm.

The L^* range was referenced from the range of the binary classification line obtained using SVM.

In Eq. (4), we substitute the pupil diameter r , which linearly changes between 6 mm and 8 mm for $L^* \geq 25$, the surrounding luminance $L' = 0.11 \text{ cd/m}^2$, when displaying $(R, G, B) = (0, 0, 0)$, and the surrounding radius $A = 20 \text{ mm}$ when considering a circle cut out of a blackout curtain as the extended light source projected on the retina. Figure 11 shows the functions obtained by further substituting the luminance and radius of reference points 1, 2, and 3 into the resulting equation, which is plotted in black in Fig. 8. Fig. 11(a), (b), and (c) correspond to reference point 1, 2, and 3, respectively.

The similarity between the binary classification line, which indicates the threshold for points perceived to be closer or farther than the reference points, and the function showing the relationship between L^* and the viewing angle when the retinal illuminance is equal to that of the reference point, suggests that the level of retinal illuminance may determine the depth perception of small-field light sources. Since the values of retinal illuminance, area of the image projected onto the retina, including the surroundings of small-field light source and pupil diameter are based on assumptions, there is a need for verification through accurate measurements. Assuming that the depth and the magnitude of retinal illuminance determine the perception of small-field light sources, and the observers' pupil sizes were measured, the identical retinal illuminance function obtained can accurately determine depth.

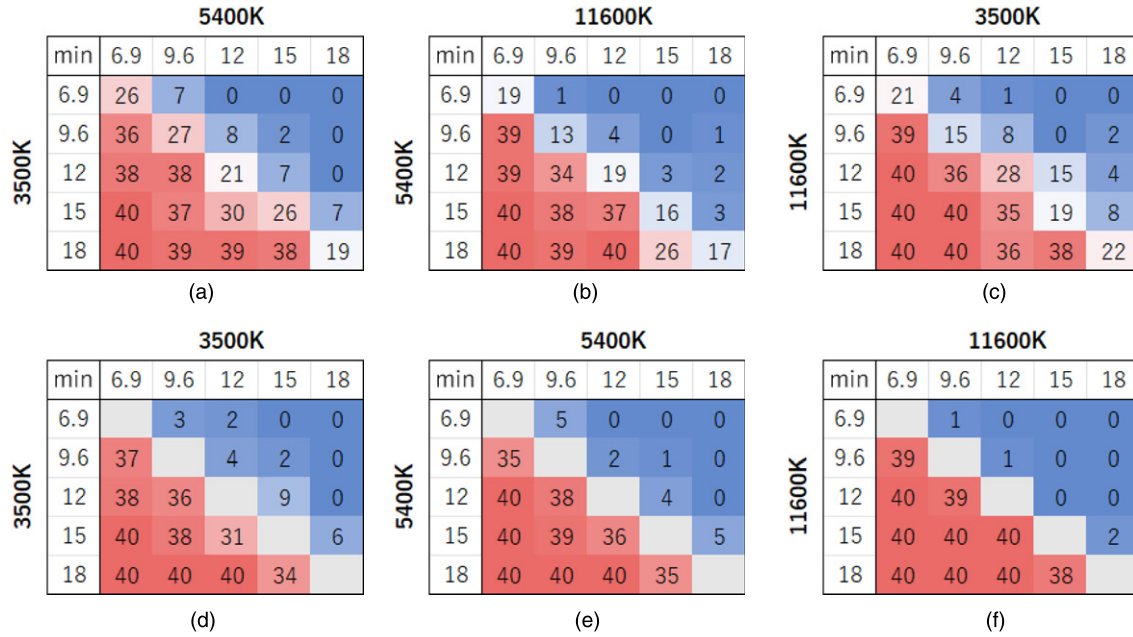


Figure 12. Result of Experiment 2, Stimulus 1. (a) 3500 K versus 5400 K. (b) 5400 K versus 11600 K. (c) 11600 K versus 3500 K. (d) 3500 K versus 3500 K. (e) 5400 K versus 5400 K. (f) 11600 K versus 11600 K.

4.2 Experiment 2: Color

4.2.1 Results

Figure 12 summarizes the results for ten observers exposed to Stimulus 1. “Min” represents the five viewing angles noted in Table II(a). The numbers in the table represent the number of times an observer selected the color temperature indicated on the vertical axis as being perceived to be in front compared to the color temperature indicated on the horizontal axis, with values ranging from 0 to 40 for all combinations of small-field light sources. Frequent selections are shown in red and infrequent selections are shown in blue. Fig. 12(a) illustrates that when comparing the depths of two points which are (color temperature (K), viewing angle (min)) = (3500, 6.9) and (color temperature (K), viewing angle (min)) = (5400, 6.9), the number of times that “(color temperature (K), viewing angle (min)) = (3500, 6.9) is in front” was chosen 26 times from a total of 40. The diagonals in these tables are blank as they were not compared with small-field light sources of same size, luminance, or color temperature.

Figure 13 summarizes the results for ten observers exposed to Stimulus 2, where L^* represents L^* values shown in Table II(b). The values in the table are the same as those in Stimulus 1 and take values from 0 to 40 for all combinations of small-field light sources. There was no correlation between visual acuity and the results for either stimulus.

4.2.2 Considerations

The observations for pairs of equal-color temperatures, such as 3500 K versus 3500 K, 5400 K versus 5400 K, and 11600 K versus 11600 K show that the characteristics of the retinal image size and light attenuation, which are depth cues, are at work. In other words, for all color temperatures (3500,

Table III. Difference between theoretical value, Stimulus 2.

	3500 K	5400 K	11600 K
Size and color temp.	52	34	8
Lum. and color temp.	38	24	10

5400, and 11600 K), a larger image was perceived to be in front when size alone was different, and a brighter image was perceived in the foreground when the luminance alone was different.

However, when the difference in size or luminance between two experimental stimuli was small, a smaller or darker stimulus was occasionally selected as the foreground stimulus. Assuming that only retinal image size and light attenuation are involved in depth perception and that there is no noise, the results are likely to be as shown in Figure 14. Selections that deviate from the characteristics of depth cues are attributed to noise or confusion in depth perception, as retinal image size and light attenuation make it difficult to perceive distance. Table III and Fig. 14 elucidate the observations for pairs with same color temperature (Fig. 12(d), Fig. 12(e), Fig. 12(f), Fig. 13(d), Fig. 13(e), and Fig. 13(f)), and the sum of the absolute values of the differences for the corresponding components. It can be concluded that the lower the color temperature, the more significant the difference, regardless of whether the size or luminance changes. Therefore, if noise, such as selection errors and individual differences, is constant at all color temperatures, a lower color temperature is associated with a higher likelihood of confusion in depth perception.

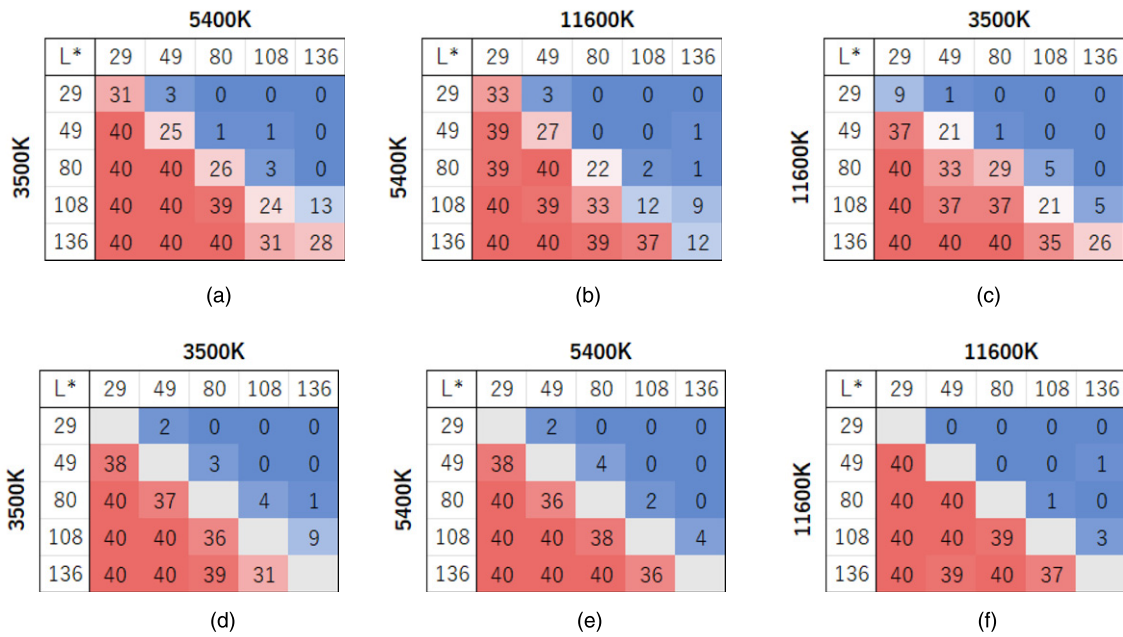


Figure 13. Result of Experiment 2, Stimulus 2. (a) 3500 K versus 5400 K. (b) 5400 K versus 11600 K. (c) 11600 K versus 3500 K. (d) 3500 K versus 3500 K. (e) 5400 K versus 5400 K. (f) 11600 K versus 11600 K.

Table IV. Wilcoxon signed-rank test. (a) Observations pertaining to Stimulus 1. (b) Observations pertaining to Stimulus 2.

(a)			
	3500 K versus 3500 K	5400 K versus 5400 K	11600 K versus 11600 K
3500 K versus 5400 K	0.164	0.105	
5400 K versus 11600 K		0.110	0.221
11600 K versus 3500 K	0.041		0.095

(b)			
	3500 K versus 3500 K	5400 K versus 5400 K	11600 K versus 11600 K
3500 K versus 5400 K	0.007	0.021	
5400 K versus 11600 K		0.726	0.917
11600 K versus 3500 K	0.909		0.730

Bevan et al. posited that red and yellow were overestimated in size compared to green and blue [1], while Shahidi et al. indicated that lower color temperatures increased perceived brightness [17]. Considering these findings, it is possible that the lower color temperatures led to less accurate size perception and appeared relatively darker, leading to a confusion in depth perception.

Table IV(a) summarizes the p-values calculated from Wilcoxon signed-rank test, corresponding to the results of pairs with different and same color temperatures, as shown in Fig. 12. Table IV(b) also corresponds to Fig. 13. Tests between results unrelated to the control experiment were not conducted; therefore, these cells are blank.

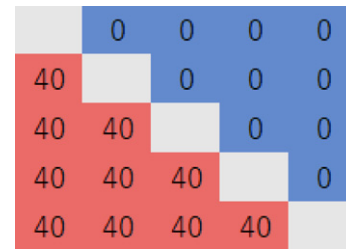


Figure 14. Theoretical value.

It is evident that only 3500 K versus 5400 K for Stimulus 2 differed significantly from 3500 K versus 3500 K and 5400 K versus 5400 K at 5% significance level. These results indicate that color, a depth cue, has a minor effect compared with retinal image size and light attenuation cues. However, results with p-values above 5% significance level do not indicate that color has no impact; therefore, we analyzed the effect of color by focusing on the diagonal components of experimental results.

The values of diagonal components are pairs of points of equal size and luminance that differ only in terms of color temperature. If color does not affect depth perception, the diagonal component is likely to be 20 and the median of the possible range is 0–40. Figure 15 shows only the diagonal components, Fig. 15(a) corresponds to Fig. 13, Stimulus 1, and Fig. 15(b) corresponds to Fig. 14, Stimulus 2.

It can be inferred that for 3500 K versus 5400 K, 3500 K was more likely to be perceived to be in front than 5400 K, and the difference in luminance was more sensitive to this effect than the difference in size. For 5400 K versus 11600 K, 5400 K was more likely to be perceived in front if luminance was low, and 11600 K was more likely to be

Viewing Angle (min)	6.9	9.6	12	15	18
3500K>5400K	26	27	21	26	19
5400K>11600K	19	13	19	16	17
11600K>3500K	21	15	28	19	22

(a)

L^*	29	49	80	108	136
3500K>5400K	31	25	26	24	28
5400K>11600K	33	27	22	12	12
11600K>3500K	9	21	29	21	26

(b)

Figure 15. Diagonal component of Experiment 2 results. (a) Components of Stimulus 1. (b) Components of Stimulus 2.

perceived in the foreground if luminance is high. As shown in Table II(a), for Stimulus 1, L^* was fixed at 89.8. Therefore, when cross-referenced with Fig. 15, it can be inferred that the depth perception thresholds for 5400 and 11600 K are within the L^* range of 80–90. For 11600 K versus 3500 K, no specific trend was observed for either Stimulus 1 or Stimulus 2.

In general, color advancement occurs in the order of red > yellow > green > blue wavelengths as a depth cue [6, 7]. Furthermore, during twilight or scotopic vision, the maximum visual sensitivity shifts towards shorter wavelengths, resulting in Purkinje effect [18], where red appears darker than blue. This phenomenon may be related to light attenuation or to depth perception, which is influenced by light attenuation. However, these characteristics were obtained mainly through experiments of illuminating non-luminescent colored surfaces, and different characteristics are likely to be obtained when observing light sources with chromaticity directly. Indeed, the absence of a specific trend between 3500 K on long-wavelength and 11600 K on short-wavelength contradicts the color advance-recession or Purkinje phenomenon.

Based on the results of this experiment, it can be hypothesized that points with higher luminance tend to be perceived as closer to the observer for both 3500 K and 11600 K compared to 5400 K. Therefore when comparing two points with similar hues, it is possible that higher saturation points are more likely to be perceived to be closer. The reversal of 5400 K versus 11600 K results at the point of low luminance may indicate the confusion of four observers, who reported that between 5400 K and 11600 K they saw only two different colors, white and orange (warm colors) for the stimulus colors used in experiments. Ogawa et al., in their study on point-light source color perception, reported that a higher color temperature is associated with a wider color discrimination threshold [14]. There is a possibility that at points with particularly low luminance, 5400 K appeared to have higher saturation than 11600 K. To verify this hypothesis, color-matching experiments are needed for small-field light sources in dark viewing with different sizes and luminance. Deciphering depth perception

between 3500 K and 11600 K, which are far apart in hue, can be achieved by subdividing the size and luminance steps.

5. CONCLUSIONS

This study analyzed the depth perception of ‘small-field light sources’ in one eye through 2AFC experiments to investigate depth perception when observing star images. We focused on three depth cues: retinal image size, light attenuation, and color. We investigated the effects of each cue in small-field light sources and their interrelationships to determine which cues influence depth perception between small-field light sources.

Experiment 1 was a comparison of the depth perception of achromatic points of varying sizes and luminance. Using a reference point with a fixed viewing angle and luminance and 100 comparison points with randomly determined values, we determined the threshold of the comparison points perceived to be positioned in the foreground and background. The experimental results suggest that retinal image size and light attenuation are depth cues in small-field light sources, and that the interaction between them may be explained by retinal illuminance. Experiment 2 introduced three color temperatures (3500, 5400, and 11600 K). Depth comparisons were made between points of different sizes and color temperatures as well as between points of different luminance and color temperatures. We set five levels of luminance for each color temperature and analyzed the influence of color on depth perception by comparing all point combinations. Significant insights were gained from the experiments. First, lower color temperatures tend to cause more confusion in depth perception owing to the size of the retinal image and light attenuation. Moreover, the influence of color on depth perception is minimal. Finally, when comparing two points with similar hues, the point with higher saturation tended to be perceived as slightly closer.

The hypothesis made in Experiment 1 that the interrelationship between the size and luminance of small-field light sources in depth perception can be explained by retinal illuminance is yet to be fully validated owing to the lack of accurate measurements of pupil diameter and peripheral brightness calculations. Therefore, it is necessary to modify experimental methods and verify our hypotheses. In Experiment 2, introducing color temperatures other than 3500, 5400, and 11600 K may yield more accurate data. In addition, it is necessary to investigate the viewing angle and luminance discrimination threshold of small-field light sources at different color temperatures, considering that size and luminance perception may differ depending on the color. We compared only two small-field light sources in this study, but night sky displays countless stars. Therefore, it is necessary to verify whether the results of this study are applicable when the number of small-field light sources increases. By conducting studies that simulate real-world conditions, such as point clouds resembling the Milky Way or the appearance of exceptionally bright objects such as the moon nearby, it is anticipated that achieving a more authentic reproduction of the night sky is feasible.

ACKNOWLEDGMENT

This study was supported by JSPS KAKENHI (Grant Number 20H05958).

REFERENCES

- ¹ W. Bevan and W. F. Duk, "Color as a Variable in the Judgment of Size," *Am. J. Psychol.* **66**, 283–288 (1953).
- ² J. C. Bradley, K. C. Bentley, A. I. Mughal, H. Bodhireddy, and S. M. Brown, "Dark-adapted pupil diameter as a function of age measured with the NeuroOptics pupillometer," *J. Refractive Surg.* **11**, 202–207 (2011).
- ³ R. C. Carter and L. D. Silverstein, "Size matters: improved color-difference estimation for small visual targets," *J. Soc. Inf. Disp.* **18**, 17–28 (2010).
- ⁴ F. Chéreau, "Stellarium," <https://stellarium.org/ja/>, (2024).
- ⁵ DarkSky International, "Losing the Dark," <https://darksky.org/resources/videos/losing-the-dark/>, (2023).
- ⁶ S.-M. Gong, F.-Y. Liou, and W.-Y. Lee, "The effect of lightness, chroma, and hue on depth perception," *Color Res.* **48**, 793–800 (2023).
- ⁷ C. R. C. Guibal and B. Dresp, "Interaction of color and geometric cues in depth perception: When does 'red' mean 'near'?", *Psychological Res.* **69**, 30–40 (2004).
- ⁸ A. Ichikawa, S. Saida, A. Osa, and K. Munechika, "Integration of binocular disparity and monocular cues at near threshold level," *Vis. Res.* **43**, 2439–2449 (2003).
- ⁹ F. E. L. Jamiy and R. Marsh, "Survey on depth perception in head mounted displays: distance estimation in virtual reality, augmented reality, and mixed reality," *IET Image Process.* **13**, 707–712 (2019).
- ¹⁰ E. B. Johnston and B. G. Cumming, "Integration of depth modules: stereopsis and texture," *Vis. Res.* **33**, 813–826 (1993).
- ¹¹ M. S. Landy, L. T. Maloney, E. B. Johnston, and M. Young, "Measurement and modeling of depth cue combination: in defense of weak fusion," *Vis. Res.* **35**, 389–412 (1995).
- ¹² M. Luckiesh, "On 'Retiring' and 'Advancing' Colors," *Am. J. Psychol.* **29**, 182–186 (1918).
- ¹³ K. J. McCree, "Small-field tritanopia and the effects of voluntary fixation," *Int'l. J. Opt.* **7**, 317–323 (1960).
- ¹⁴ R. Ogawa, M. Tanaka, and T. Horiuchi, "Colour perception of LED point light sources in scotopic vision," *CIE 2021 Conf.* (Kuala Lumpur, Malaysia, Vienna, Austria: CIE, 2021), pp. 104–110.
- ¹⁵ S. Palmisano, B. Gillam, D. G. Govan, R. S. Allison, and J. M. Harris, "Stereoscopic perception of real depths at large distances," *J. Vis.* **10**, 1–16 (2010).
- ¹⁶ K. Sawada, F. Nakayama, and M. Okyudo, "Empirical study on the sigital planetarium system for measuring visual perception of the night sky: analysis of impact from light pollution and astourism," *Res. Appl.* **33**, 52–61 (2023).
- ¹⁷ R. Shahidi, R. Golmohammadi, M. Babamiri, J. Faradmal, and M. Aliabadi, "Effect of warm/cool white lights on visual perception and mood in warm/cool color environments," *EXCLI J.* **20**, 1379–1393 (2021).
- ¹⁸ J. C. Shin, H. Yaguchi, and S. Shioiri, "Change of color appearance in photopic," *Mesopic and Scotopic Vis., Opt. Rev.* **11**, 265–271 (2004).
- ¹⁹ J. Stare, "Light pollution map," <https://www.lightpollutionmap.info/>, (2024).
- ²⁰ M. Tanaka, T. Horiuchi, K. Otani, and P. Hung, "Evaluation for faithful reproduction of star fields in a planetarium," *J. Imaging Sci. Technol.* **61**, 1–12 (2017).
- ²¹ M. Tanaka, T. Horiuchi, and K. Otani, "Relationship between faithfulness and preference of stars in a planetarium," *J. Perceptual Imaging* **2**, 1–11 (2019).
- ²² M. Tanaka, K. Otani, S. Setoguchi, and T. Horiuchi, "The reproduction and evaluation of star fields with the Milky Way in a planetarium," *Appl. Sci.* **11**, 1413–1426 (2021).
- ²³ H. H. Telek, H. Erdol, and A. Turk, "The effects of age on pupil diameter at different light amplitudes," *Beyoglu Eye J.* **3**, 80–85 (2018).
- ²⁴ E. Wolf, *Progress in Optics* (Elsevier, Amsterdam, 2008), p. 349.